Optimizing In-motion Wireless Charging Service Efficiency for Electric Vehicles: A Game Theoretic Approach

Li Yan and Haiying Shen
Department of Computer Science
University of Virginia, USA
Email: {ly4ss, hs6ms}@virginia.edu

***Abstract*—With the application of Wireless Power Transfer (WPT) techniques for Electric Vehicles (EVs), public transportation EVs are expected to be continuously operable without recharging downtime. A road segment equipped with an in-motion wireless charger is called a charger lane. To maximize the service efficiency of deployed in-motion wireless chargers without suffering from traffic congestion, we must properly manage the traffic of the EVs and coordinate their arrivals at the charger lanes to avoid the generation of traffic congestion at the charger lanes and on the road segments to them. In this paper, we propose *WPT-Opt*, a game theoretic approach for Optimizing in-motion wireless charging service efficiency, minimizing EVs' time spent on the way to the charger, and avoiding traffic congestion at the charger lanes, to fulfill this task. We studied a metropolitan-scale dataset of public transportation EVs, and observed the EVs' spatial and temporal preference in selecting chargers, competition for chargers during busy charging times, and the relationship between vehicle density and driving velocity on a road segment. Then, we formulate a non-cooperative Stackelberg game between all the EVs and a *central controller*, in which each EV aims at minimizing its charging time cost to its selected target charger, while the *central controller* tries to maximally avoid the generation of congestion on the in-motion wireless chargers and the road segments to them in the near future. Our trace-driven experiments on SUMO demonstrate that *WPT-Opt* can maximally reduce the average charging time cost of the EVs by approximately 200% during different hours of a day.**

I. INTRODUCTION

Due to foreseen depletion of fossil fuels, many countries are actively adopting Electric Vehicles (EVs) for public transit systems [1]. The public service EVs (e.g., taxicabs, buses) are expected to keep driving without a long period of recharge downtime, although they only have limited driving range (e.g., 200 km) due to battery capacity. Wireless Power Transfer (WPT) techniques for in-motion EV charging [2], [3] and the deployment of in-motion wireless chargers (wireless chargers in short) [4] provide a solution to the above expectation. A road segment equipped with a wireless charger is called a charger lane. However, an EV may suffer from traffic congestion (i.e., long driving time) on the way to its selected target charger or long non-charging time at the charger without recharge (non-charging time in short). EV charging scheduling system should ensure the chargers' service efficiency (i.e., as many charged EVs as possible per unit time and each passed EV can be fully charged) [5].

Many scheduling strategies of EVs for improving the service efficiency of plug-in charging stations have been proposed [5]–[12]. Generally, they recommend target charging stations, which result in the minimum charging time cost (i.e., charger seeking time before reaching their target charging station plus non-charging (waiting) time at the charging station), to EVs based on current status of charging stations (e.g., location, number of available chargers). However, their charging time cost is estimated based on current traffic status. If the availability (i.e., number of available chargers) of the target charging station or the traffic on the road segments to the station changes, the EVs may suffer from traffic congestion and a long charging time cost. What's more, these methods are not applicable for in-motion wireless chargers due to different charging approaches. For example, before busy charging times, the chargers may be non-congested. However, if legions of EVs drive to the currently "optimal recommended wireless charger lane" (i.e., the wireless charger lane with the shortest estimated charging time cost), they may crowd into the wireless charger lane or the road segments connecting the chargers simultaneously. Such competition for the wireless charger lane may result in traffic congestion. Since congestion will greatly decrease EVs' passing velocity at the wireless charger lane [2], it will result in less EVs passing through the charger lane during a unit time (i.e., degraded charger service efficiency).

However, the solution is non-trivial. Most charger deployment methods (including plug-in and in-motion wireless chargers) [4], [13]–[15] advocate deploying plug-in chargers to the positions with high volume of EV traffic to offer easy access for EVs. However, the chargers deployed at these positions may frequently suffer from traffic congestion. The road congestion on a wireless charger lane is measured by its vehicle density (i.e., number of vehicles per unit length); a higher vehicle density increases the service efficiency of the charger lane but generates congestion and decreases vehicle velocity, and vice versa. Therefore, it is a challenge to maximize the service efficiency of a network of wireless chargers while proactively avoiding the generation of congestion at the chargers and on the road segments to them. Accordingly, we aim to propose a game theoretic wireless charging service efficiency optimization strategy to handle this challenge.

After an EV sends out a charging request, it reports its information (e.g., velocity, current position, target charger lane) to a *central controller* (e.g., hosted in the cloud or fog) periodically (e.g., every 5 minutes) until it arrives at its target charger lane. Non-electric vehicles and other EVs without charging request also periodically report their current driving information to the *central controller* for vehicle density estimation of the road segments. We aim to avoid traffic congestion on the road segments connecting the positions of the EVs that have charging request and the EVs' target wireless chargers. We call the collection of these road segments *road segment set*. The *central controller* then utilizes each EV's trajectory (that connects the origin and its target charger lane) in the next time slot and determines the parameters (e.g., EV density of the road segments in *road segment set*, expected EV driving velocity) depicting the future service efficiency of the wireless chargers. This is based on the observation that a vehicle's trajectory can soundly illustrate its future mobility [16]–[19]. To maximize the service efficiency of the wireless chargers while avoiding EV congestion on them and the road segments to them, the *central controller* formulates a non-cooperative Stackelberg game, in which each EV aims at minimizing the charging time cost to its target charger lane, while the *central controller* tries to maximize the service efficiency of all the wireless chargers. That is, each EV always wants to drive by its expected fastest velocity, but may neglect the potential risk of traffic congestion, which conflicts with the the *central controller*, which wants to maximize the service efficiency of the wireless chargers and vehicle flow rate (i.e., average number of vehicles per unit time) of the road segments to them. After the Stackelberg equilibrium is reached, when the EVs follow their optimal velocities (i.e., fastest velocity without causing traffic congestion), the service efficiency of the wireless chargers and the vehicle flow rate of the road segments to them are maximized. In summary, our contributions include:

(1) Our analysis on a metropolitan-scale EV mobility dataset confirms the movement and charging characteristics of EVs, and lays the foundation for the design of *WPT-Opt*.
(2) We propose a wireless charging service efficiency optimization strategy that utilizes a non-cooperative Stackelberg game between the *central controller* and all EVs to minimize each EV's charging time cost, and meanwhile maximize the service efficiency of wireless chargers.
(3) We have conducted extensive trace-driven experiments to show the effectiveness of *WPT-Opt* in terms of the number of charged EVs per unit time, the charging time cost of the EVs, and vehicle density on the wireless chargers. Compared with previous methods, *WPT-Opt* can maximally reduce the average charging time cost of the EVs by approximately 200% during different hours of a day.

To our knowledge, this paper is the first work for optimizing the service efficiency of wireless chargers from the perspective of avoiding EV traffic congestion in the future. The remainder of the paper is organized as follows. Section II presents literature review. Section IV presents our dataset analysis results. Section V presents the detailed design of *WPT-Opt*. Section VI presents performance evaluations. Section VII concludes the paper with remarks on future work.

II. Related Work

EV scheduling methods. Ma *et al.* [6] proposed to schedule EVs to under-utilized plug-in charging stations with reduced charging price to meet the respective charging demand of each EV and avoid extreme charging load on the power grid. Gan *et al.* [7] further predict the peak electricity-using hours of EVs at charging stations, and reduce the price of recharging for each EV to avoid extreme charging load. Sundstrom *et al.* [12] proposed to minimize the cost of electricity and overload on the power grid through personalizing a charging plan (i.e., when and where to charge) for each EV. Kim *et al.* [11] proposed to rank EVs' charging requests by arrival time and estimated charging delay, and schedule the EVs to charging stations by their ranks to reduce the EVs' non-charging time. Qin *et al.* [10] and Lu *et al.* [9] considered the remaining power of EVs, and the number of available chargers in charging stations to minimize the EVs' non-charging time. Malandrino *et al.* [8] modeled EVs' charging behavior (e.g., where and when to charge) and availability of charging stations with game theory to find the optimal charging price of each charging station that balances the charging load. Tian *et al.* [5] proposed to use each EV's historical recharging events, real-time trajectories and current traffic state to recommend the EV a charging station that leads to the minimal charging time cost. However, these methods are not directly applicable for wireless chargers because they cannot avoid the generation of traffic congestion on the recommended charger lane or on the road segments to the charger lane in the near future, which may severely degrade the service efficiency of a charger lane.

Vehicle future mobility based routing. Wu *et al.* [16] found the spatio-temporal correlation in vehicle mobility and noted that the future trajectory of a vehicle is correlated with its past trajectory. In Trajectory-based Data Forwarding Scheme (TBD) [17], Trajectory-based Statistical Forwarding Scheme (TSF) [18] and Shared-Trajectory-based Data Forwarding Scheme (STDFS) [19], trajectory information of vehicles is collected through access points and used to predict vehicle mobility for data forwarding. Our work is based on the observations that trajectories illustrate vehicles' future mobility, which can be used to estimate future road vehicle density.

III. Background and Motivation

A. Definitions and Preliminaries

A *road network* is a directed graph, in which vertices represent landmarks (i.e., intersections or turning points), and edges represent road segments connecting the landmarks [20]. We have the following definition for a vehicle trajectory.

Definition 1. Trajectory. *V_i's trajectory consists of the a start position P_i^s, an end position P_i^e and a sequence of time-ordered landmarks,*
$\Phi_i^l : \{P_i^s, (p_0, t_0), \ldots, (p_j, t_j), \ldots, (p_{N_i^l-1}, t_{N_i^l-1}), P_i^e\}$,
where p_j is a landmark's GPS position. N_i^l is the total number of landmarks covered by this trajectory.

A vehicle's movement record is continuous. As in [20], if a vehicle has stayed at a stop position for a long period of time (e.g., 10 minutes), we determine that the vehicle has finished its previous trajectory. Thus, such stop positions cut the vehicle's continuous movement into several trajectories.

B. Vehicle Flow Rate and Velocity at Chargers Matters

Vehicle density of a road segment s_i, (denoted by d_i) is defined as the average number of vehicles per mile in the road segment (veh/mile), and the vehicle flow rate of s_i (denoted by r_i) is defined as the average number of vehicles driving through s_i per unit time [20], [21]. That is, the vehicle flow rate of s_i equals to the product of vehicle density and average vehicle passing velocity on s_i (denoted by v_i): $r_i = d_i \cdot v_i$. Moreover, the amount of energy transferred to an EV from a wireless charger lane is dependent on the EV's passing velocity [2], [3]. Each wireless charger lane has a specified EV passing velocity v_i'. An EV will be fully charged only when it drives through the charger lane with a velocity equal to or lower than v_i'. Also, since different EVs have different battery capacities, their full recharge time for the same charger lane will be different. To ensure that all the EVs can be fully charged, we use the maximum battery capacity of the EVs to determine the v_i' of each charger lane. Therefore, we can see that to maximize the service efficiency of a wireless charger lane, we need to increase the vehicle flow rate at the charger lane and the road segments to it as much as possible, and meanwhile ensure that the EVs will pass the charger lane with the charger's specified velocity.

IV. Metropolitan-Scale Dataset Measurement

A. Dataset Description and Data Processing System

Our datasets are collected from Shenzhen, China (1.1–12.31, 2015), with a recording period of 30 seconds:

1. **Taxicab Dataset.** It is collected by the Shenzhen Transport Committee, which records the status (e.g., timestamp, position, velocity, SoC status) of 15,610 taxicabs, among which 6,510 of them are EVs.
2. **Dada Car Dataset.** It is provided by the Dada Car corporation (a customized transit service similar to UberPool), which records the status (e.g., timestamp, position, velocity) of 12,386 electric reserved service vehicles.
3. **Road Map.** The road map of Shenzhen is obtained from OpenStreetMap [22]. According to the municipal information of Shenzhen [1], we use a bounding box with coordinate $(lat = 22.4450, lon = 113.7130)$ as the south-west corner, and coordinate $(lat = 22.8844, lon = 114.5270)$ as the north-east corner, which covers an area of around 2,926km^2, to crop the road map data.
4. **Charging Station Dataset.** It is also collected by the Shenzhen Transport Committee, which records the information (e.g., GPS position, number of chargers) of 81 existing plug-in charging stations in Shenzhen. The number of chargers in the charging stations ranges from 4 to 28. The charging stations are open to all EVs.

B. Dataset Analysis

In the data analysis, we only selected the movement records of electric taxicabs and Dada cars for data analysis. We directly use the method introduced in [5] to determine whether an EV is approaching its target charging station, recharging at the station or leaving the station. Specifically, if an EV's movement record shows that it has stayed at a charging station for a long period of time (e.g., 10 minutes), we consider that it was recharging at the station at that time. Therefore, the charger seeking time before reaching the EV's target charging station is defined as the time interval between the time that the EV decides to have a recharge and the time it enters the target charging station for a recharge; the non-charging time of the EV at the target charging station is defined as the time duration it stays at the charging station but is not receiving recharge. Although our dataset analysis is applied on plug-in charging stations, we believe that the collected results are

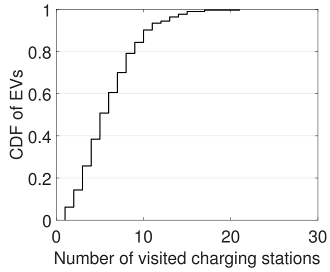

Fig. 1: Frequently visited charging stations of all vehicles.

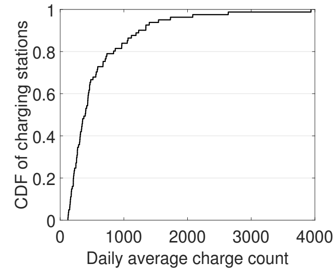

Fig. 2: Distribution of daily average charge counts of all charging stations.

representative under the case of wireless chargers, since the EVs' long-term pattern (e.g., frequently driven road segments, working hours) remains relatively stable.

1) EVs' Spatial Preference on Chargers: The charge count of a charging station is defined as the number of EVs that charged at this charging station. It was indicated that an EV may have its own spatial preference in selecting charging stations [5]. In this analysis, we attempt to verify if the difference in the preference of selecting charging stations is conspicuous among different EVs, and the charging popularity (i.e., daily average charge count of EVs) differs significantly among different charging stations.

We measured the number of charging stations an EV visited more than 1 time per day in average throughout 2015. Figure 1 shows the results. We can see that 80% of the EVs only charged at less than 10 charging stations per day in average. For the rest 20%, the maximum number of visited charging stations is only around 20. This means that EVs have quite stable preference in selecting charging stations. If many EVs charge at the same charging stations, they may cause congestion at these charging stations or the road segments to them.

We further measured the total daily average charge count of all the charging stations. Figure 2 shows the Cumulative Density Function (CDF) of the results. We can see that only 20% of the charging stations have a daily average charge count higher than 1,000. But the highest value can be as high as around 4,000. The charging station with the highest value has 28 chargers. This result confirms that the charging stations have different levels of popularity among the EVs. The competition of the EVs for popular charging stations must be avoided to prevent the generation of possible congestion, which will result in long non-charging time of the EVs.

2) EVs' Temporal Preference on Chargers: The busy charging times (i.e., hours with relatively more charge counts) of the charging stations may also be quite different. To confirm this, we randomly selected three charging stations and measured the daily average charge count during each hour of a day throughout 2015. Figure 3 shows the measured results. We can see that for Station 0 (16 chargers), its busy charging time happens between 06:00 and 10:00; for Station 1 (10 chargers), its busy charging time happens between 08:00 and 20:00; and for Station 2 (19 chargers), its busy charging time happens between 10:00 and 14:00.

To explicitly illustrate the difference between the busy charging times of the charging stations, we further measured the maximum daily average charge count of each charging station and its corresponding hour. Figure 4 shows the mea-

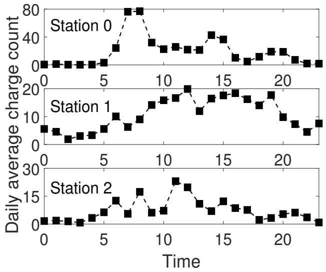

Fig. 3: Temporal preference on three charging stations.

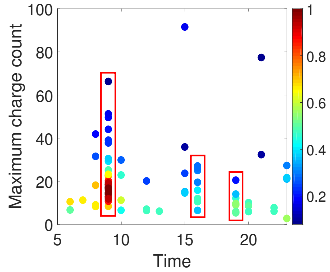

Fig. 4: Scatter plot of maximum charge count vs. corresponding time.

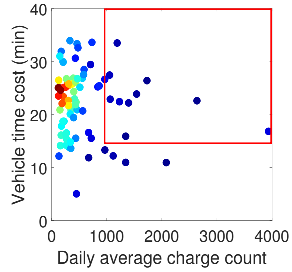

Fig. 5: Competition for charging stations.

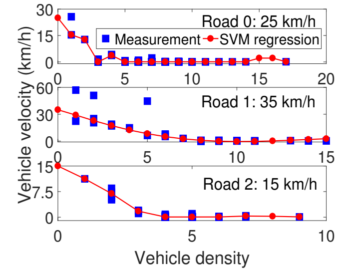

Fig. 6: Relation between vehicle density and actual driving velocity.

sured results with a density scatter heat plot between the maximum number of charge count of each charging station and its corresponding time. Each point represents a charging station. The warmer color a point has, the more concentrated it is with other points, which have similar metric values. We can see that most busy charging times happen at around 09:00, 16:00 and 19:00 (i.e., points surrounded by red squares). These results illustrate that for different charging stations, their busy charging times are different, and their maximum charge counts are also quite different. To identify whether such charging counts will degrade the service of some charging stations, we further investigated the competition for chargers among EVs.

3) Competition for Chargers Among EVs: Previous methods schedule EVs based on current status of EV traffic and current availability of charging stations. If an EV's velocity is individually optimized without considering other EVs' future mobility, many EVs may crowd into some charging stations or road segments to them and generate congestion. To illustrate this problem, we measured the daily average charge count and the average vehicle charging time cost to each of the 81 charging stations. The results are illustrated in Figure 5 with a density scatter heat plot. We can see that most charging stations (i.e., points with the warmest colors) have a relatively low daily average charge count (i.e., $<$100), but a relatively high vehicle charging time cost (i.e., $\approx$25 minutes). This is because that they are relatively distant to the areas that the EVs frequently visit, so the EVs need to drive a long time to reach them. However, we still see that for a few charging stations marked by the red square, they are frequently visited by the EVs (i.e., $>$1000), but result in long charging time costs for the EVs (i.e., $>$15 minutes). This result confirms that EVs do have competition for certain charging stations.

4) Relation between Vehicle Density and Driving Velocity on A Road Segment: It has been indicated that vehicles' actual driving velocity on a road segment is subject to the vehicle density of the road segment [23]. However, previous work has demonstrated that the accurate relation between the actual vehicle driving velocity and the vehicle density of a road segment cannot be modeled with a parametric function (e.g., linear function) [24]. Support Vector Machine Regression (SVMR) is effective in learning the nonlinear relation between several variables [25]. For each road segment, we may use its historical records of vehicle density and vehicle passing velocity during a period (e.g., 15 minutes) to train the SVMR model and use the learned relation function to estimate the actual vehicle driving velocity given its vehicle density.

We randomly selected three road segments, of which velocity limits are 25 km/h, 35 km/h and 15 km/h, and measured the vehicle density and average vehicle passing velocity with a period of 15 minutes from July 1 to July 31 in 2015. These road segments are potentially suitable for deploying wireless charger lanes according to previous charger lane deployment works [4] due to their relatively slow vehicle passing velocities. But such road segments are more prone to traffic congestion than others if without a proper traffic control mechanism due to their narrow road width and slow EV passing velocity. Then, for each road segment, we feed its measured results to the SVMR model to learn the relation function between its vehicle density and actual vehicle driving velocity. The results are illustrated in Figure 6. We can see that for the three road segments, the actual vehicle driving velocity generally decreases as the vehicle density increases, but with different decreasing rates. Also, the SVMR results fit the historical records with acceptable precision. In Section V-B2, we will elaborate how we use the estimated actual vehicle driving velocity to calculate the travel time of a vehicle trajectory and predict a road segment's future vehicle density.

V. System Design Details

A. System Overview

WPT-Opt consists of two parts: *All EVs* as the service follower and a *central controller* (e.g., hosted in cloud or fog) as the service provider, which outputs charging service information to the EVs. The system structure is shown in Figure 7. Above all, we have the following assumptions:

1. Each EV who has charging request will firstly use previous methods [5]–[12] to determine its *target charger lane*. Meanwhile, it is willing to report and adjust its *driving status (current position, velocity)* according to the charging service information.
2. Non-electric vehicles and EVs without a charging request are also willing to report their current driving trajectory to the *central controller* for vehicle density estimation. This is reasonable because that these vehicles can receive better routing benefit from providing such information.

In Section IV-B, we have demonstrated that *all EVs* have their respective spatial and temporal preference on selecting charging stations, and such preferences can cause competition. To let *all EVs* reach their *target charger lane* as fast as possible, and meanwhile maximize the service efficiency of wireless chargers without generating congestion, we use the Stackelberg game [21] between the EVs and the *central controller* to determine the expected vehicle density that maximizes the service efficiency of the wireless chargers and

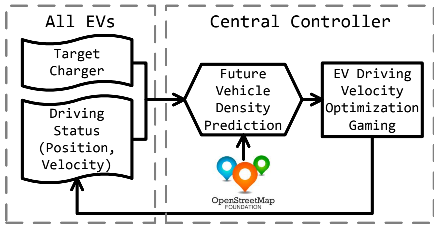

Fig. 7: System structure.

the optimal driving velocity for each EV. Specifically, the EVs report its *driving status (current position, velocity)* to the *central controller* periodically (e.g., every 5 minutes). In response, the *central controller* outputs the optimized driving velocity for each EV periodically. At the start of current time slot $\mathcal{T}_c$ (e.g., 5 minutes), the *central controller* applies the *future vehicle density prediction* (Section V-B) on the *road segment set* (i.e., the set of road segments connecting the positions of the EVs with a charging request and the EVs' target chargers) for the next time slot $\mathcal{T}_{c+1}$:

1. Each EV keeps reporting its *driving status (current position, velocity)* and *target charger lane* to the *central controller*.
2. Based on the information collected from the EV, the *central controller* calculates its trajectory travel time in $\mathcal{T}_{c+1}$ to know the EV's possible position in any time during $\mathcal{T}_{c+1}$. Then the *central controller* aggregates the trajectories and predicts the vehicle density of each road segment in $\mathcal{T}_{c+1}$.

By the end of current time slot $\mathcal{T}_c$, an *EV driving velocity optimization gaming* (Section V-C) is conducted between the *central controller* and all the EVs. The gaming process is executed periodically with a time interval $\mathcal{T}$ (e.g., 5 minutes):

1. Based on the predicted average vehicle density over all the road segments in *road segment set* in $\mathcal{T}_{c+1}$, the *central controller* determines a set of candidate expected average vehicle densities over the next time slot for the *road segment set*, which are achievable by vehicle velocity adjustment.
2. Based on each expected average density, each EV determines its actual driving velocity on its current road segment and reports it to the *central controller*.
3. The *central controller* determines the final expected average density that maximizes the service efficiency of wireless chargers and the vehicle flow rate of the road segments connecting the chargers, and notifies all the EVs.
4. Each EV chooses its velocity corresponding to the final expected average density.

We first explain how the *central controller* predicts the vehicle density of road segments (Section V-B), and then present the non-cooperative Stackelberg gaming (Section V-C).

B. Future Vehicle Density Prediction

To make the gaming process work after each time slot $\mathcal{T}$ (e.g., 5 minutes), we must be able to calculate the future vehicle density of wireless chargers and the road segments to them. To this end, we must solve the following problems:

1. How to estimate the travel time to each road segment of an EV's future trajectory based on the current vehicle density of each road segment (i.e., $\mathcal{T}_c$)? (Section V-B1)
2. How to utilize the future trajectories and the travel times to the road segments of the trajectories of all the EVs to predict the future vehicle density of each road segment in the next time slot (i.e., $\mathcal{T}_{c+1}$)? (Section V-B2)

1) Trajectory Travel Time Calculation: With the current position and target charger lane periodically reported by each EV, the *central controller* uses an existing routing method (e.g., [5]) to determine the EV's trajectory in the next time slot $\mathcal{T}_{c+1}$, which is a sequence of road segments connecting the EV's current position and target charger lane. Note that other non-electric vehicles and EVs without a charging request also report their current driving trajectories to the *central controller*. It then utilizes the combination of all the trajectories to calculate the travel time of each road segment that will be passed in $\mathcal{T}_{c+1}$ by the EV. In our gaming process, we will determine a vehicle's actual driving velocity (v_i) on a road segment (s_i). Then, for each s_i, the estimated travel time on s_i (denoted by $\widetilde{t_i}$) is $\widetilde{t_i} = l_i/v_i$, where l_i is the length of s_i.

In Section IV-B4, we have shown that the actual vehicle driving velocity v_i of a road segment s_i is related to its vehicle density d_i, and the relation is relatively stable but non-parametric, which is denoted as $v_i = f_i(d_i)$. SVMR model is effective in estimating the non-parametric function between two variables [25]. Thus, for each road segment, we build its SVMR model to learn its relation between v_i and d_i. Specifically, we input its vehicle density as the predictor value and the corresponding actual vehicle driving velocity as the response value to the SVMR model. The output is the estimated relation function between the vehicle density and the actual vehicle driving velocity of the road segment. Later, given an estimated vehicle density of the road segment, we can use the function to output its actual vehicle driving velocity, and further estimate the travel time of the road segment.

Several previous works [26], [27] have confirmed that the travel time of a road segment can be described by normally distributed and statistically independent random variables with acceptable precision. Therefore, for an EV, we estimate its travel time of the trajectory from its current position to s_i as the sum of the travel times of the road segments included in the trajectory, $\widetilde{T_i} = \sum_{k=1}^{M_i} \widetilde{t_k}$, where M_i is the number of the road segments included in the trajectory. Based on the historical records of the travel time of road segment s_k from all vehicles, the *central controller* can calculate the variance of s_k's travel time σ_k^2 for each composing road segment. Then, the standard deviation of $\widetilde{T_i}$ is calculated by summing the variances of the composing road segments, $\Delta_i^2 = \sum_{k=1}^{M_i} \sigma_k^2$. This is because that $\widetilde{t_k}$ follows normal distribution. Finally, an EV's trajectory can be represented as a sequence of road segments it will pass in $\mathcal{T}_{c+1}$ and their corresponding estimated travel times $\{(s_i, \widetilde{T_i}) | i = 1, 2, \ldots, M\}$, where M denotes the total number of road segments that the EV will pass in $\mathcal{T}_{c+1}$.

2) Road Vehicle Density Calculation: Due to the inaccuracy of the above estimation, the estimated travel time in $\{(s_i, \widetilde{T_i}) | i = 1, 2, \ldots, M\}$ has a certain probability to be accurate. That is, each vehicle only has a certain probability to appear on a road segment at the estimated travel time. Then, we use the probabilities of all the vehicles to calculate the vehicle density of each road segment in $\mathcal{T}_{c+1}$. Specifically, we first calculate the probability that a vehicle will appear at each road segment in its trajectory in $\mathcal{T}_{c+1}$. Then, we sum up all the vehicles' appearance probabilities at a road segment in $\mathcal{T}_{c+1}$ as the vehicle density of the road segment in $\mathcal{T}_{c+1}$.

Given the next time slot $\mathcal{T}_{c+1} = [t^s_j, t^e_j]$ (e.g., [00:00,00:05]), where j means it is the jth time slot in a day, t^s_j and t^e_j are the start time and end time of the time slot, respectively. The *central controller* then measures each vehicle's appearance probability at s_i during $[t^s_j, t^e_j]$ by referring to the vehicle's estimated travel time to s_i. Therefore, we can calculate the vehicle's appearance probability at s_i during $[t^s_j, t^e_j]$ as

$$P(T_i \leqslant t^e_j - t^s_j) = \Phi(\frac{t^e_j - t^s_j - \widetilde{T}_i}{\Delta_i}) - \Phi(\frac{-\widetilde{T}_i}{\Delta_i}) \quad (1)$$

where T_i denotes the EV's actual travel time from current position to s_i, and $\Phi(\cdot)$ is the CDF of the standard normal distribution with mean $\widetilde{T}_i$ and standard deviation Δ_i. Based on the historical records of all vehicles' travel time on s_i, we can calculate the CDF of the travel time on s_i. By summing up the appearance probabilities of the vehicles on s_i during $\mathcal{T}_{c+1}$, the *central controller* estimates the vehicle density of each s_i in $\mathcal{T}_{c+1}$ as:

$$d^{s_i}_{c+1} = \sum_{k=1}^{N} P_k(T_i \leqslant t^e_j - t^s_j) \quad (2)$$

where N is the number of EVs that will pass s_i during $[t^s_j, t^e_j]$.

C. EV Driving Velocity Optimization Gaming

1) Overview: We refer to a previous work on traffic optimization [28] for the establishment of the Stackelberg game. In the Stackelberg game, the service leader (i.e., *central controller*) considers the predicted average vehicle density of a road segment, and then chooses a set of expected vehicle densities, D={$d_1, d_2, ..., d_n$}, that are achievable by vehicle velocity adjustment. The *central controller* hopes to evenly distribute the EVs over *road segment set* by properly assigning a d value. The EV drivers receive D from the *central controller* and picks a velocity in response to each d_i to maximize its own utility (driving as fast and safely as possible while minimizing the risk of congestion). Next, the *central controller* selects the vehicle density, which is denoted by d_l, that maximizes the service efficiency of the wireless chargers and vehicle flow rate of the road segments connecting them, and then the EVs choose their velocities corresponding to the selected d_l. Finally, we solve the Stackelberg equilibrium of the game, i.e., the game reaches a state that the service efficiency of wireless chargers is maximized while the EV drivers are satisfied with the driving status (judged by driving velocity and associated risk of congestion). The gaming is executed periodically. In the following, we first introduce the utility of an EV driver and the utility of the *central controller*, and then introduce the gaming between them.

2) Utility Function of EV Drivers: For EV drivers, we define a utility function as the level of benefit an EV driver can obtain through driving by a certain velocity on road segment s_i. An EV driver can receive more benefit (i.e., arrive at its target charger lane earlier than expected) if it drives at a relatively higher velocity. However, as discussed in Section I, if all EVs drive at their fastest velocities, their risk of suffering from congestion may increase. Therefore, we formulate an EV driver's utility function as a value calculated by subtracting the potential risk of congestion ($U_r(\cdot)$) from the driver's satisfaction degree ($U_s(\cdot)$) resulted from driving fast, as shown in Equation (3).

$$\begin{aligned} F(v_i, \alpha_i) &= U_s(v_i, \alpha_i) - U_r(d, v_i) \\ \text{s.t.} \quad v_i &\leqslant v_i^{max} \end{aligned} \quad (3)$$

where v_i is the vehicle's velocity for optimization, which is selected by the vehicle itself; α_i is a scale factor to make $U_s(\cdot)$ and $U_r(\cdot)$ comparable.

Specifically, an EV driver's satisfaction degree $U_s(\cdot)$ is primarily determined by its driving velocity [21]. $U_s(\cdot)$ ought to be non-decreasing as each driver desires high velocity (i.e., short driving time to its target charger lane). Also, $U_s(\cdot)$ should reach the largest value only when the vehicle is driving at the velocity corresponding to the vehicle density expected by the *central controller*, which is denoted as $f_i(d)$. Meanwhile, the derivative of the satisfaction degree is non-increasing because the driver's satisfaction degree gradually gets saturated when the vehicle velocity increases to some level [23]. Considering these properties, we design $U_s(\cdot)$ as a concave function. Since the Natural Logarithmic Functions are representative concave functions [29], we define:

$$U_s(v_i, \alpha_i) = \alpha_i \cdot \ln(v_i). \quad (4)$$

An EV driver's potential risk of congestion is closely related to its vehicle flow rate [21]. As the EV is expected to drive by the velocity corresponding to the d (i.e., $f_i(d)$), we use a Sigmoid function to approximate the probability of congestion with respect to the EV's selected driving velocity. If the EV drives above the threshold $f_i(d)$, the probability of congestion increases significantly. Therefore, we formulate an EV driver's potential risk of congestion as

$$U_r(d, v_i) = \frac{1}{1 + e^{-(v_i - f_i(d))}} dv_i \quad (5)$$

As the EV increases its velocity, its utility will firstly increase to the maxima at some velocity around $f_i(d)$, and then decrease. Thus, the EV's velocity is adjusted by the *central controller*, and meanwhile can drive by a relatively fast velocity. Combining Equation (4) and Equation (5) into Equation (3), we have:

$$\begin{aligned} F(v_i, \alpha_i) &= \alpha_i \cdot \ln(v_i) - \frac{1}{1 + e^{-(v_i - f_i(d))}} dv_i \\ \text{s.t.} \quad v_i &\leqslant v_i^{max} \end{aligned} \quad (6)$$

3) Utility Function of Central Controller: The *central controller* always aims at maximizing EV flow rate on wireless chargers and the road segments connecting them. Also, recall that each wireless charger lane has a specified EV passing velocity v'_i, which enables the wireless charger lane to fully charge the EV after driving through the charger lane (Section III-B). Correspondingly, the utility function of the *central controller* is defined as:

$$L(d) = \sum_{i=1}^{N_s} d_i \cdot v_i + \sum_{i=1}^{N_e} d_i \cdot v_i \cdot e^{-|v_i - v'_i|} \quad (7)$$

where N_s is the total number of road segments excluding the wireless chargers in *road segment set*; N_e is the total number of wireless chargers; Recall that in Section III-B, we have explained that an EV will be fully charged only when it drives through the wireless charger lane with a velocity equal to or lower than the charger lane's specified EV passing velocity v'_i. Considering that we also expect EVs to pass through a wireless charger lane as fast as possible, we use the $e^{-|v_i - v_i'|}$ on the utility part of wireless chargers to specify that the *central controller* expects the EVs to pass through each wireless charger lane at their specified EV passing velocity v_i'. A passing velocity other than this value will result in a utility loss for the *central controller*.

4) Optimal Driving Velocity Selection: Recall that based on Equation (2), the *central controller* predicts the vehicle densities of all wireless chargers and the road segments to them. It then calculates the average estimated vehicle density of the wireless chargers and the road segments connecting them during next period of gaming: $\overline{d_{c+1}} = \sum_{k=1}^{N_s} d_{c+1}^{s_k}/N_s + \sum_{k=1}^{N_e} d_{c+1}^{s_k}/N_e$. Based on $\overline{d_{c+1}}$, the *central controller* determines a range of expected vehicle densities that are achievable by vehicle velocity adjustment, and offers these densities to each vehicle for selection, which is defined as:

$$d_u = \ln(u+1) \cdot \overline{d_{c+1}},\ u \in [1, ..., n] \tag{8}$$

We use D=$\{d_1, d_2, ..., d_n\}$ to denote the n levels of expected vehicle densities for $\mathcal{T}_{c+1}$. In practice, n should be at least larger than the exponential constant (i.e., $n \geqslant e \approx 2.718$) so that the vehicle has multiple selections around $\overline{d_{c+1}}$. The *central controller* notifies drivers of the D. If $\overline{d_{c+1}}$ leads to an increased expected vehicle density (d_u), it means some EVs will suffer from a higher risk of traffic congestion if they all keep their current velocity. According to Equation (6), to maintain the highest utility $F(v_i, \alpha_i)$, the EV drivers will decrease driving velocity. Otherwise, the EV drivers' risk of encountering traffic congestion will be lower, which enables the drivers to increase driving velocity to maintain the highest utility $F(v_i, \alpha_i)$. Note that the increment rate of $U_s(\cdot)$ (Natural Logarithmic Function) is slower than $U_r(\cdot)$ (product of Sigmoid Function and Linear Function) when velocity v_i increases. Therefore, according to Equation (3), increasing driving velocity on current road segment (v_i) will reduce a driver's utility because $U_r(\cdot)$ will increase faster than $U_s(\cdot)$. Thus, driving at a slower velocity can prevent the vehicle density of the wireless chargers and the road segments connecting them from further increasing.

For each $d_u \in D$, if a driver will drive in its current road segment s_i during the next time slot, it chooses a new velocity that maximizes its utility $F(\cdot)$, denoted by v_{iu}:

$$v_{iu} = \mathop{\arg\max}_{v_i \leqslant v_i^{max}} F(v_i, \alpha_i) \tag{9}$$

If a driver will drive through more than one road segment s_i, s_j,..., it chooses a set of velocities in each of the segments to maximize its utility $F(\cdot)$, denoted by $\{v_{iu}, v_{ju}, ...\}$ as shown in Equation (10).

$$\{v_{iu}, v_{ju}, ...\} = \mathop{\arg\max}_{v_k \leqslant v_k^{max}} \sum_k \gamma_k F(v_k, \alpha_k) \tag{10}$$

Finally, the driver reports the n candidate velocities to the *central controller*. To maximize its utility $L(\cdot)$ based on the candidate velocities from all drivers, the *central controller* determines the expected vehicle density (d_l):

$$d_l = \mathop{\arg\max}_{d_u \in D} L(d_u) = \mathop{\arg\max}_{d_u \in D} d_u \sum_{N_s} v_{iu} \tag{11}$$

The *central controller* then uses the d_l as the new expected vehicle density and notifies it to all the drivers. Then, each driver picks the optimal velocity corresponding to d_l from the n candidate velocities.

VI. Performance Evaluation

A. Comparison Methods

To evaluate *WPT-Opt*'s performance, we compare it with a representative charging station recommendation system [5] (*Recommend* in short), and a baseline method, in which each EV selects the nearest charging station for recharge (*Baseline* in short). To make the methods comparable, they all use the same deployment of wireless chargers based on the existing positions of charging stations. In *Recommend*, when an EV sends out a request for recharging, the *central controller* calculates the non-charging time of each existing charging station based on current occupancy of the charging station, and the charger seeking time based on current traffic. Finally, the *central controller* outputs the charging station with the minimal charging time cost. While in *Baseline*, whenever an EV requests a recharge, the *central controller* recommends it the charger lane with the shortest driving time. Note that the calculation of the driving time does not consider current traffic state on road network. In *WPT-Opt*, we assume that the target charger lane of the EVs are determined by the *central controller* with the same method of *Recommend* based on current traffic status and charger availability.

B. Experiment Settings

We set the charger lane length at each charging position to be 1 km [2]. The battery capacities of the EVs follow a uniform distribution between 32 kWh and 37 kWh, which is the common battery capacity of public service EVs in Shenzhen [1]. The charging rate of a charger lane is 150 kW [2]. This means that each EV needs around 900 seconds (0.25 hours) to get a full recharge. That is, the specified EV passing velocity of a wireless charger lane (v_i' in Equation (7)) is 1 km/0.25 hours=4 km/h. We use SUMO [30] to simulate 10,000 EVs on Shenzhen's road network for 24 hours. We set the SoC threshold to be 20%. It is determined so that an EV is able to use its residual SoC to reach its nearest charger lane [1], [4]. When the SoC of an EV is lower than the threshold, it will send a charging request to the *central controller*. We suppose that every EV starts driving with a random SoC value higher than the threshold at the beginning of a day.

The metrics we measured are:

- *Average non-charging time of EVs*. For each EV, we measure its non-charging time at the chargers from 00:00 to 23:00. Then, we take the average non-charging time over all the EVs. We also measure the CDF of the non-charging time of each recharge. We measure this to compare the methods' performance in reducing the EVs' non-charging time.
- *Average charger seeking time of EVs*. For each EV, we measure its charger seeking time to its target charger from 00:00 to 23:00. Then, we take the average charger seeking time over all the EVs. We also measure the CDF of the charger seeking time of each recharge of all the EVs. We measure this metric to compare the methods' performance in reducing the EVs' charger seeking time.

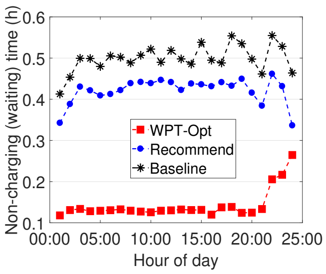

Fig. 8: Average non-charging time of all EVs per hour.

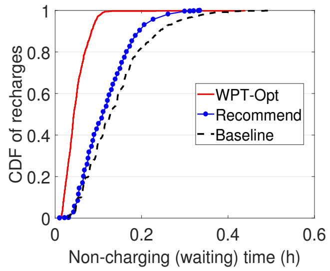

Fig. 9: Distribution of non-charging time of all EVs' recharges.

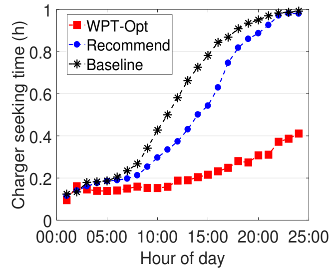

Fig. 10: Average charger seeking time of all EVs per hour.

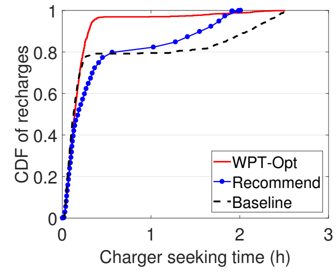

Fig. 11: Distribution of charger seeking time of all EVs' recharges.

- *Average number of charged EVs*. We measure the total number of charged EVs per hour during a day. We also measure the CDF of the charge counts of all the EVs. We measure this metric to compare the methods' performance in maximizing the service efficiency of all wireless chargers.
- *Average vehicle flow rate of all road segments*. We measure the average vehicle flow rate of all road segments per hour during a day. We measure this metric to compare the methods' performance in avoiding traffic congestion.

C. Experimental Results

1) Average Non-charging Time of EVs: Figure 8 shows the average non-charging time of all the EVs per hour under different methods. Figure 9 shows the CDF of the non-charging time of each recharge of all the EVs. We can see that the results follow: *WPT-Opt*<*Recommend*<*Baseline*.

Baseline always has the highest result during all times. This is because that it does not consider the possible generation of congestion at the chargers after determining the target charger. When an EV arrives at a charger lane, there will usually be several other EVs that have arrived at the charger lane prior to its arrival and generate congestion. Therefore, the EV has to wait until the other congested EVs finish their recharging, which greatly increases the EV's non-charging time before recharge. This is also verified in Figure 9. We can see that the non-charging time of most recharges in *Baseline* ($> 80\%$) is longer than 0.1 hours. Considering that an EV will look for a recharge whenever its SoC is below 50%, and it only takes 450 seconds to recharge 50% of the EV battery, we conclude that most EVs in *Baseline* are influenced by congestion.

In *Recommend*, the average non-charging time of the EVs per hour of day and the CDF of the non-charging time are quite approximate to those in *Baseline*. These results demonstrate that *Recommend* is ineffective in preventing congestion at the chargers. This is because that it makes the recommendation without considering the future change of charger availability and the traffic change on the road segments to the charger lane. Thus, its estimated future EV arrivals at the charger lane is not accurate, which may cause traffic congestion at the charger lane or on the way to the charger lane.

The EVs' non-charging time in *WPT-Opt* is much shorter than that in the other methods. This is because that *WPT-Opt* can utilize the EVs' trajectories to estimate the future vehicle density at the chargers, and has a game theoretic approach to avoid the generation of traffic congestion at the chargers and meanwhile enable the EVs to drive by their expected velocity.

2) Average charger seeking Time of EVs: Figure 10 shows the average charger seeking time of all the EVs per hour under different methods. We can see that during most time intervals, the results follow: *WPT-Opt*<*Recommend*<*Baseline*. Figure 11 shows the CDF of the charger seeking time of each recharge of all the EVs. We can see that around 80% of the recharges have similar charger seeking time among different methods, but the other 20% of the recharges follow: *WPT-Opt*<*Recommend*<*Baseline*.

WPT-Opt always has the shortest charger seeking time. Before optimization, the future vehicle density on the predetermined driving route has been deduced by the *central controller* from the EVs' trajectories. Thus, *WPT-Opt* enables the *central controller* to maximally avoid road congestion caused by competition on certain road segments. Meanwhile, each EV can drive by a velocity as fast as possible. As a result, *WPT-Opt* generates the shortest charger seeking time.

Recommend has the second shortest charger seeking time to target chargers during most time intervals. However, during the time intervals between 04:00 and 09:00, the EVs' charger seeking time in *Recommend* is even longer than that in *Baseline*. This is because that the controller selects the route with the minimum vehicle density and the charging station with available charging point based on current vehicle density on the road network and current availability of the charging stations. Since the selected driving route and charging station are not guaranteed to be free from traffic congestion, especially during rush hours, the EVs are sometimes delayed by traffic congestion generated in the near future.

Baseline usually has the longest charger seeking time. This is because that it does not have any approach to avoid the road segments and chargers that may suffer from traffic congestion. We can see that its charger seeking time increases enormously after 09:00, and can be as long as 2.5 hours. These results demonstrate how bad the traffic congestion can degrade the fulfillment of EVs' charging requests.

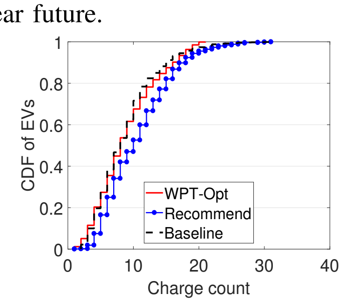

Fig. 12: Distribution of charge counts of all EVs.

3) Average Number of Charged EVs: Figure 12 shows the CDF of the charge counts of all the EVs under different methods. Figure 13 shows the total charging load created by the recharges of all the EVs per hour under different methods. We can see that the charge counts of the EVs and the charging

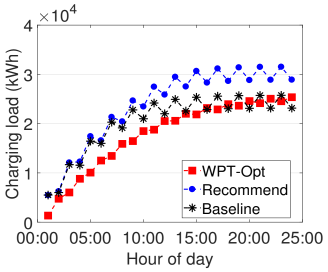

Fig. 13: Total charging load of all chargers per hour.

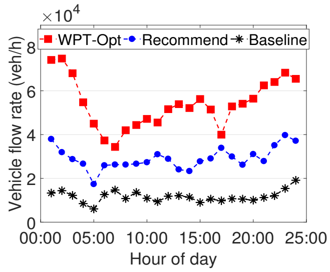

Fig. 14: Average vehicle flow rate of all road segments per hour.

load of the chargers are quite similar to each other. These results show that all the methods have served the charging demands of EVs, but with different time costs. Considering that *WPT-Opt* has a much shorter charging time cost, these results demonstrate that *WPT-Opt* can achieve a much higher wireless charger service efficiency.

4) Average Vehicle Flow Rate of All Road Segments: Figure 14 shows the average vehicle flow rate of all the road segments per hour under different methods. We can see the results follow: *WPT-Opt*>*Recommend*>*Baseline*. These results are generally consistent with those demonstrated in Figure 8 and Figure 10 due to the same reasons. It shows that *WPT-Opt* can effectively avoid the generation of traffic congestion at wireless chargers and the road segments to them.

VII. Conclusion

To maximize the service efficiency of wireless chargers, we must properly coordinate EVs' traffic and their arrival at the chargers to avoid traffic congestion at the chargers and on the road segments to them. Our proposed approach, *WPT-Opt*, is the first work that maximizes the service efficiency of wireless chargers without generating congestion, and meanwhile minimizes the EVs' charging time cost before charging. Our data analysis results confirm that EVs have spatial and temporal preference on selecting chargers, and such preferences can lead to competition for chargers. We also analyzed the relation between vehicle density and vehicles' actual driving velocity on a road segment. Supported by these results, we formulate a non-cooperative Stackelberg game between all the EVs and a *central controller*, in which each EV aims at minimizing its charging time cost to its target charger lane, while the *central controller* tries to maximally avoid the generation of congestion on wireless chargers and the road segments to them. Our trace-driven experiments on SUMO demonstrate that *WPT-Opt* can maximally reduce the average charging time cost of the EVs by approximately 200% over comparison methods. In the future, we plan to consider more EV charging behavior factors (e.g., different charging time and target charger lane in weekday and weekend).

Acknowledgements

This research was supported in part by U.S. NSF grants NSF-1827674, CCF-1822965, OAC-1724845, CNS-1733596, and Microsoft Research Faculty Fellowship 8300751.

References

[1] L. Yan, H. Shen, Z. Li, A. Sarker, J. A. Stankovic, C. Qiu, J. Zhao, and C. Xu, "Employing opportunistic charging for electric taxicabs to reduce idle time," *ACM IMWUT*, vol. 2, no. 1, 2018.

[2] Y. J. Jang, E. S. Suh, and J. W. Kim, "System architecture and mathematical models of electric transit bus system utilizing wireless power transfer technology," *Systems Journal*, 2015.

[3] A. Karalis, J. D. Joannopoulos, and M. Soljačić, "Efficient wireless non-radiative mid-range energy transfer," *Annals of Physics*, 2008.

[4] L. Yan, H. Shen, J. Zhao, C. Xu, F. Luo, and C. Qiu, "CatCharger: Deploying wireless charging lanes in a metropolitan road network through categorization and clustering of vehicle traffic," in *Proc. of INFOCOM*, 2017.

[5] Z. Tian, T. Jung, Y. Wang, F. Zhang, L. Tu, C. Xu, C. Tian, and X.-Y. Li, "Real-time charging station recommendation system for electric-vehicle taxis," *IEEE TITS*, vol. 17, no. 11, 2016.

[6] Z. Ma, D. Callaway, and I. Hiskens, "Decentralized charging control for large populations of plug-in electric vehicles," in *Proc. of CDC*, 2010.

[7] L. Gan, U. Topcu, and S. H. Low, "Optimal decentralized protocol for electric vehicle charging," *IEEE TPS*, vol. 28, no. 2, 2013.

[8] F. Malandrino, C. Casetti, and C.-F. Chiasserini, "A holistic view of its-enhanced charging markets," *IEEE TITS*, vol. 16, no. 4, 2015.

[9] J.-L. Lu, M.-Y. Yeh, Y.-C. Hsu, S.-N. Yang, C.-H. Gan, and M.-S. Chen, "Operating electric taxi fleets: A new dispatching strategy with charging plans," in *Proc. of IEVC*, 2012.

[10] H. Qin and W. Zhang, "Charging scheduling with minimal waiting in a network of electric vehicles and charging stations," in *Proc. VIN*, 2011.

[11] H.-J. Kim, J. Lee, G.-L. Park, M.-J. Kang, and M. Kang, "An efficient scheduling scheme on charging stations for smart transportation," in *Proc. of SEUCSG*, 2010.

[12] O. Sundström and C. Binding, "Planning electric-drive vehicle charging under constrained grid conditions," in *Proc. of POWERCON*, 2010.

[13] S. Bae and A. Kwasinski, "Spatial and temporal model of electric vehicle charging demand," *TSG*, 2012.

[14] Y. Zheng, Z. Y. Dong, Y. Xu, K. Meng, J. H. Zhao, and J. Qiu, "Electric vehicle battery charging/swap stations in distribution systems: comparison study and optimal planning," *TPS*, 2014.

[15] W. Yao, J. Zhao, F. Wen, Z. Dong, Y. Xue, Y. Xu, and K. Meng, "A multi-objective collaborative planning strategy for integrated power distribution and electric vehicle charging systems," *TPS*, 2014.

[16] Y. Wu, Y. Zhu, and B. Li, "Trajectory improves data delivery in vehicular networks," in *Proc. of INFOCOM*, 2011.

[17] J. Jeong, S. Guo, Y. Gu, T. He, and D. H. Du, "Trajectory-based data forwarding for light-traffic vehicular ad hoc networks," *TPDS*, vol. 22, no. 5, 2011.

[18] J. Jeong, S. Guo, Y. Gu, T. He, and D. H. Du, "Trajectory-based statistical forwarding for multihop infrastructure-to-vehicle data delivery," *TMC*, vol. 11, no. 10, 2012.

[19] F. Xu, S. Guo, J. Jeong, Y. Gu, Q. Cao, M. Liu, and T. He, "Utilizing shared vehicle trajectories for data forwarding in vehicular networks," in *Proc. of INFOCOM*, 2011.

[20] Y. Zheng, "Trajectory data mining: an overview," *TIST*, 2015.

[21] N. Groot, B. De Schutter, and H. Hellendoorn, "Toward system-optimal routing in traffic networks: a reverse stackelberg game approach," *IEEE TITS*, vol. 16, no. 1, 2015.

[22] "Openstreetmap," http://www.openstreetmap.org/, accessed in Jan, 2019.

[23] Y. Xu, Q.-J. Kong, S. Lin, and Y. Liu, "Urban traffic flow prediction based on road network model," in *Proc. of ICNSC*, 2012.

[24] Q.-J. Kong, Q. Zhao, C. Wei, and Y. Liu, "Efficient traffic state estimation for large-scale urban road networks," *IEEE TITS*, vol. 14, no. 1, 2013.

[25] H. Drucker, C. J. Burges, L. Kaufman, A. J. Smola, and V. Vapnik, "Support vector regression machines," in *Proc. of NIPS*, 1997.

[26] R. Li, H. Chai, and J. Tang, "Empirical study of travel time estimation and reliability," *Mathematical Problems in Engineering*, 2013.

[27] R. Li, G. Rose, and M. Sarvi, "Using automatic vehicle identification data to gain insight into travel time variability and its causes," *JTRB*, 2006.

[28] L. Yan and H. Shen, "TOP: vehicle trajectory based driving speed optimization strategy for travel time minimization and road congestion avoidance," in *Proc. of MASS*, 2016.

[29] K. G. Binmore, *Mathematical Analysis: a straightforward approach*. Cambridge University Press, 1982.

[30] D. Krajzewicz, J. Erdmann, M. Behrisch, and L. Bieker, "Recent development and applications of SUMO - Simulation of Urban MObility," *IJASM*, vol. 5, no. 3&4, 2012.